CHEMICAL ENGINEERING TRANSACTIONS
VOL. 41, 2014
A publication of AIDIC
The Italian Association of Chemical Engineering
www.aidic.it/cet
Guest Editors: Simonetta Palmas, Michele Mascia, Annalisa Vacca

ISBN 978-88-95608-32-7; **ISSN** 2283-9216
DOI: 10.3303/CET1441009

High Oxidation State of Iron in Molten Hydroxides

Ján Híveš*, Miroslav Gál, Kamil Kerekeš

Slovak University of Technology in Bratislava, Radlinského 9, 812 37 Bratislava, Slovakia
jan.hives@stuba.sk

The increased interest in iron in the high oxidation state 6+ arises from its potential as an environment friendly cleaner for remediation processes, as an perspective alternative for “green” battery cathodes, and as a suitable oxidant for organic synthesis. The effective synthesis of ferrates(VI) became the challenging task for several research groups all over the world. Three main methods of ferrates(VI) synthesis have been proposed: electrochemical, wet chemical and thermal method. Electrochemical one can be considered as a “green” method because no harmful and expensive chemicals to oxidize Fe to the 6+ oxidation state are used. Two main environments are suitable for ferrates(VI) electrochemical synthesis: strong alkaline aqueous solutions and molten hydroxides. The electrochemical way of ferrates(VI) production provides product of high purity. The synthesis of ferrates(VI) by an anodic dissolution of metallic iron proceeds typically in the transpassive potential region. At these conditions, the surface of the iron anode is covered by a partly disintegrated (e.g. containing cracks and/or pores) oxo-hydroxide layer. Efficiency of the synthesis is strongly influenced by the protective properties of this layer. These can be affected into a significant degree by the anode material used and/or by the reaction conditions, i.e. by the electrolyte concentration, composition, temperature and the cell arrangement.

1. Introduction

Three basic methods of ferrates(VI) preparation are reported by Macova et al. (2009). The first one is called dry oxidation or thermal method: iron or iron oxide is heated to a high temperature in the melt of alkali metal compounds (e.g. oxides, peroxides). The resulting product is corresponding ferrate(VI) of the alkali metal. The second one is so called wet oxidation: its principle is based on the absorption of chlorine in the solution of concentrated sodium hydroxide and subsequent reaction of the resulting hypochlorite ferric ion to form ferrates(VI). The last one is the electrochemical anodic dissolution (oxidation) of iron or cast iron in the concentrated hydroxide solutions or melts at proper anode potential until ferrates(VI) are obtained. There has been a gradual increase in attention to this method because it can provide solution for a majority of the problems associated with the previous ones (Sharma, 2002). In the case of the melts suitable temperature for ferrates(VI) synthesis is up to 200 ºC. In aqueous solutions the typical temperature range is from 20 to 70 °C, Macova et al. (2009). Using electrochemical methods the high purity ferrates(VI) can be prepared. However, the stability of the product in the presence of water remains the weak point of this approach especially in aqueous environment. Even a small amount of water presented in the highly alkaline paste decomposes ferrate(VI) within hours. Sharma (2002) suggested the utilization of organic medium instead of usual aqueous ones. However, the lower electrical conductivity on the one side and higher toxicity on the other side disadvantage this approach.
In this contribution the later method will be discussed. The influence of such parameters as molten salts KOH and electrode (pure iron, silicon rich steel, white cast iron) composition, and temperature on the ferrate(VI) formation will be addressed. Cyclic voltammetry and electrochemical impedance spectroscopy were chosen to characterize in details this process.

2. Materials and methods

2.1 Chemicals

Potassium hydroxides (Mikrochem Ltd., Slovakia) in p.a. grade was used to prepare electrolytes. The KOH solids were vacuum dried in an oven in the presence of P_2O_5 for at least five days at gradually increasing

Please cite this article as: Hives J., Gal M., Kerekes K., 2014, High oxidation state of iron in molten hydroxides, Chemical Engineering Transactions, 41, 49-54 DOI: 10.3303/CET1441009

temperature up to 200 °C. The differential temperature analysis (DTA) and thermal gravimetry (TG) showed a presence of ca. 1-2 % (n/n) water in hydroxide salt (Hives et al., 2006). Further determination of KOH purity was performed by acidimetric titration with HCl (Mikrochem Ltd., Slovakia, p.a.), using Methyl red indicator (Lachema, Czech Republic, p.a.). Carbonates were determined gravimetrically, by precipitation with barium chloride (Lachema, Czech Republic, p.a.).

2.2 Apparatus, electrodes and procedures

An oil thermostat with calibrated sensor, stainless steel box and PTFE crucible with the sample was used for our experiments. Reference connection of thermocouple was immersed in a Dewar flask with ice-water. Measuring connection of thermocouple was immersed into the melt at the same level as electrodes, Hrnciarikova et al. (2010).

Electrochemical measurements were performed using AUTOLAB instrument PGSTAT 20 equipped with FRA2 module (ECO Chemie, The Netherlands). A three electrode electrochemical cell was used for all experiments. Working electrodes (WE) were made from: (A) pure iron (Fe) (99.95 % (w/w) Fe, 0.005 % (w/w) C, 0.0048 % (w/w) Ni and 0.0003 % (w/w) Mn), (B) silicon steel (FeSi) (3.17 % (w/w) Si, 0.47 % (w/w) Cu, 0.23 % (w/w) Mn, 0.03 % (w/w) Ni), and (C) white cast iron (FeC) (3.17 % (w/w) C in the form of Fe3C, 0.44 % (w/w) Mn and 0.036 % (w/w) Ni). The geometric area of the working electrodes varied from 0.2 to 0.7 cm^2. The same material as WE served as the quasi reference electrode (RE). Counter electrode (CE) was made from mild steel (steel class 11). Measurements were carried out in a PTFE crucible containing the melt of 50 g ($KOH:KOH.H_2O$). The temperature was varied in the range 110 °C to 160 °C. The lower temperature was limited temperature of eutectic $KOH:KOH.H_2O$ which is 100 °C at the composition of 86.5 % (w/w).

Cyclic voltammograms were recorded in the potential range from (-0.3 to 1.8) V vs. RE using various polarization rates. Electrochemical impedance spectroscopy (EIS) measurements were carried out in the same systems immediately after the measurement of polarization curves. Prior to each EIS measurement every working electrode was polarised at certain anode potential for 5 minutes in order to obtain stationary conditions. The potential of the working electrode was gradually increased by 25 mV from 1.35 up to 1.75 V vs. RE. In this area, the formation of ferrates(VI) was expected. Frequency range used for the impedance measurements was from 10 Hz to 100 kHz. Perturbation signal had a sinusoidal shape with amplitude of 5 mV.

3. Results and discussion

In Figure 1 cyclic voltammograms of Fe, FeSi and FeC electrodes in molten KOH medium are shown.

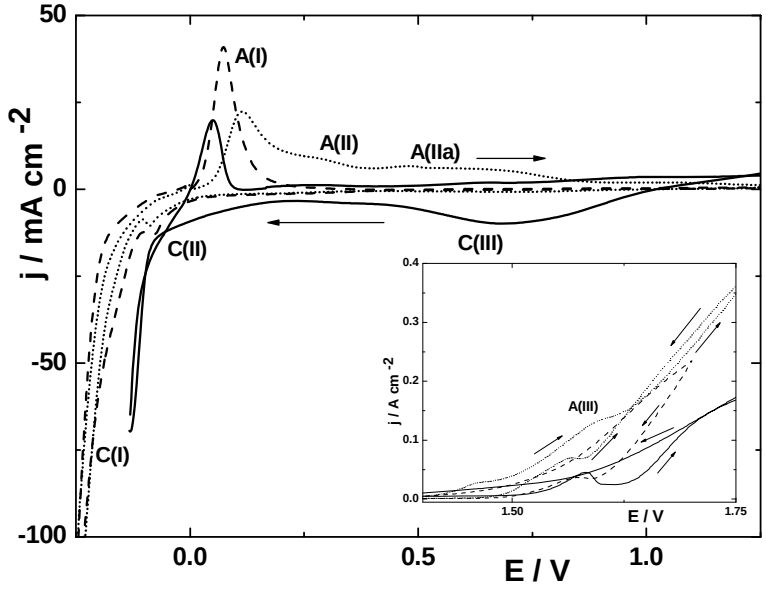

Figure 1: Cyclic voltammograms of working electrodes, i.e. pure iron (solid line), FeSi (dashed line), and FeC (dotted line) at t = 120 °C in molten KOH at scan rate of 20 mV s^{-1}; arrows indicate the potential sweep direction.

The presence of several anodic and cathodic current peaks can be seen. The intensity of peaks depends on both temperature and electrode materials used. On the anodic part of the cyclic voltammograms at temperature of 120 °C for FeC electrode two separated current peaks A(I) at around 0.15 V vs. RE, and A(II), that correspond to the Fe(II) and Fe(III) formation, respectively, are presented. On the other side, the separation of A(I) and A(II) peaks is worse for FeSi electrode, and for Fe electrode only shoulder following A(I) peak can be found. Subsequent anodic polarization leads to the A(II) peak formation (ca 300 mV more positively than A(I)). At higher temperatures (160 °C) only one, well developed, A(I) peak followed by shoulder representing A(II) peak for all three electrodes is visible. As concluded previously due to the kinetic limitation of overall process and specific insulating properties of the surface layer current peak A(II) is less visible in the case of FeSi and pure iron electrodes than A(I) one at low temperatures and for all electrodes at high temperatures (Hives et al., 2008a). After the remarkable decrease of the current densities for all three electrodes due to their pasivation, new broad, not perfectly pronounced current peak in the region (1.1 - 1.25) V vs. RE is observed. This peak, as stated before, is assigned to the transformation and restructuring of an anodic solid surface layer (Macova et al., 2010). Subsequently, after passivity region the transpassive anodic electrode dissolution, including ferrate(VI) formation followed by oxygen evolution occurs and new A(III) current peak at about 1.6 V vs. RE is formed. Only slight differences in the A(III) peak potentials are observed among electrodes. With increasing temperature the visibility of A(III) peak is getting better for all three electrodes. As in the case of molten NaOH the hysteresis in the course of voltammetric curve in the transpassive potential region was observed. At higher temperatures the peak potential of A(III) peak is slightly shifted to the more negative potentials indicating the lower energy demand for oxidation process.

In the opposite cathodic direction three peaks corresponding to three anodic peaks appeared. A broad reduction peak of ferrate(VI) (peak C(III)) occurs at potentials of 0.6 to 0.80 V vs. RE depending on both temperature and electrode material used. This peak C(III) is at all temperatures the best pronounced for Fe electrode. For both FeSi and FeC electrodes only low, broad peak is observed. In the case of FeC electrode low cathodic current peak at 1.25 V is also visible. With increasing the temperature the peak of ferrates(VI) reduction (peak C(III)) is slightly shifted to the more positive potentials indicating less energy requirement for their reduction. The highest current densities are observed for pure iron electrode. In the potential region from 0 V to 0.25 V vs. RE peaks that correspond to the reduction of Fe(III) to Fe(II) (peak C(II)) and subsequent reduction to Fe(0) (peak C(I)) are found. Both are shifted to the more negative potentials with increasing temperature for all electrodes. One can therefore conclude, that the structure of the anode plays an important role in ferrate(VI) production also in molten salts environment (Macova et al. 2010, 2011, 2012).

In the next Figure 2 the dependences of the A(III) peak current density on the square root of potential scan rate for both various materials and temperatures are plotted.

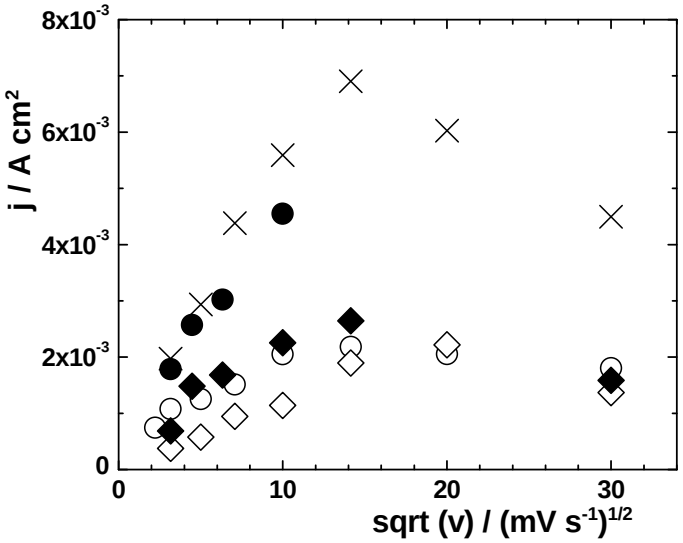

Figure 2: The dependences of the anodic peak current densities (A(III)) on the square root of potential scan rate; ○ pure Fe electrode at 110 °C; • pure Fe electrode at 160 °C; ◊ FeSi electrode at 110 °C; ◆ FeSi electrode at 160 °C; × FeC electrode at 160 °C.

For all systems the linear dependences of the current density on square root of the polarization rate in the region below 0.2 V/s were found indicating that the electrode reaction kinetic is controlled by the mass transport under the semi infinitive linear diffusion conditions (Macova et al., 2010). At higher scan rates current densities after reaching a certain maximum at about 250 mV/s decreases with further increasing of the polarization rate. Some chemical step due to the electrode structure becomes the rate determining when scan rate reach ca. 250 mV/s. Our observation is in agreement with some previous results in the hydroxide melts (Hives et al., 2010). In the strong alkaline aqueous solutions the subsequent chemical reaction was also observed (Macova et al., 2010, 2011, 2012).
EIS was also used to deeply characterize ferrate(VI) production in molten KOH because this method is suitable for properties and surface layer structure studies. Nyquist plots of impedance data obtained for FeC electrode at various potentials are shown in Figure 3.

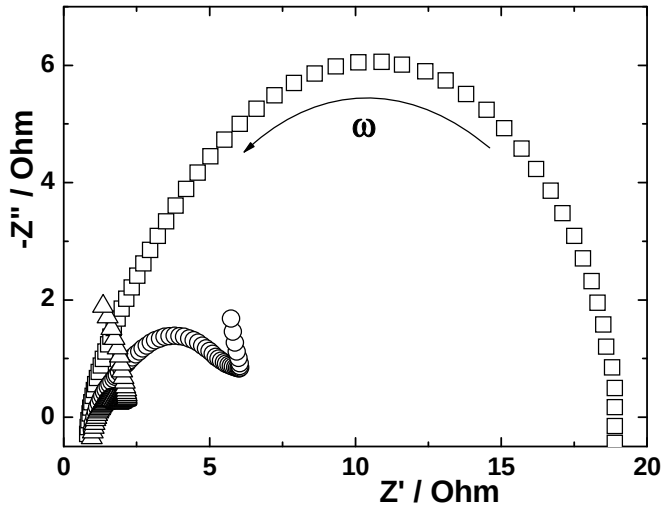

Figure 3: Nyquist plots of impedance spectra for white cast iron (FeC) electrode at t = 130 °C and at chosen potentials vs. RE: □ 1.4 V; ○ 1.5 V; Δ 1.65 V vs. RE; arrows indicate the direction of the frequency enhancement.

Two time constants can be recognized. The proposed model is based on the concept of two macrohomogeneous surface layers (Macova et al., 2010). The optimized parameters of nonlinear analysis of the equivalent circuit for white cast iron (FeC) electrode at low and high temperatures in dependence on the electrode potential are shown in Figure 4. It can be seen that resistances of both inner and outer layer decrease with increasing applied potential. Either both layers are disintegrated by strong anodic potential and/or by strong oxygen evolution or are getting thinner with increasing potential. Resistances of both outer and inner layer are approximately equal indicating the same thicker and/or compactness. Three regions are visible in these plots: short plateau at the beginning indicating stability of the individual layers at the end of the passivity region, then relatively fast decrease of the resistance of both layers meaning either reduction of the thickness or the development of the spongy or porous structures in the both layers, and at the end of measured potential second plateau that can be assigned to disrupted layers. The capacity of inner and outer layer increases with increasing potential. This is in agreement with decrease of the resistances of both layers: layers are getting thinner and/or more disintegrated by oxygen evolution or strong anodic dissolution. Capacities of inner and outer layers are slightly dependent on the temperature meaning that both layers are losing their thickness and/or compactness equally at all the temperature used.
From n parameter of the constant phase element supplementary information characterizing the surface structure of the electrode can be obtained. Similarly to the resistances, the curve of the dependence of n on E can be divided into three regions for both layers indicating the same changes in both individual layers with increasing potentials. The outer layer at lower temperature is getting porous or spongy and, vice versa, at higher temperatures becomes more ideal with increasing polarization potential. Bearing in mind the previous conclusions about R_{out} and Q_{out}, one should think about the disintegration of the outer layer rather than reduction in its thickness.
Contrary to previous observations, n_{inn} changes from quasi ideal to spongy at high temperature and to ideal at lower temperatures. Therefore, the conclusions made for R_{inn} and Q_{inn} are connected to the reduction in thickness of the inner layer rather than its disintegration especially at low temperatures.

Parameters for other two electrodes show the similar trends as in the case of FeC one (not shown). R_{inn} and R_{out} are the highest for pure iron electrode and slightly higher for FeSi than for FeC electrode. The capacities of individual layers are the highest for FeC electrode and the lowest for pure Fe electrode. Both parameters indicate that the layers are the thickest for pure iron electrode and the thinnest for FeC electrode. This statement corresponds with CV results, where C(III) peak was the highest for pure iron electrode meaning the highest amount of ferrate(VI) presented on the electrode surface.

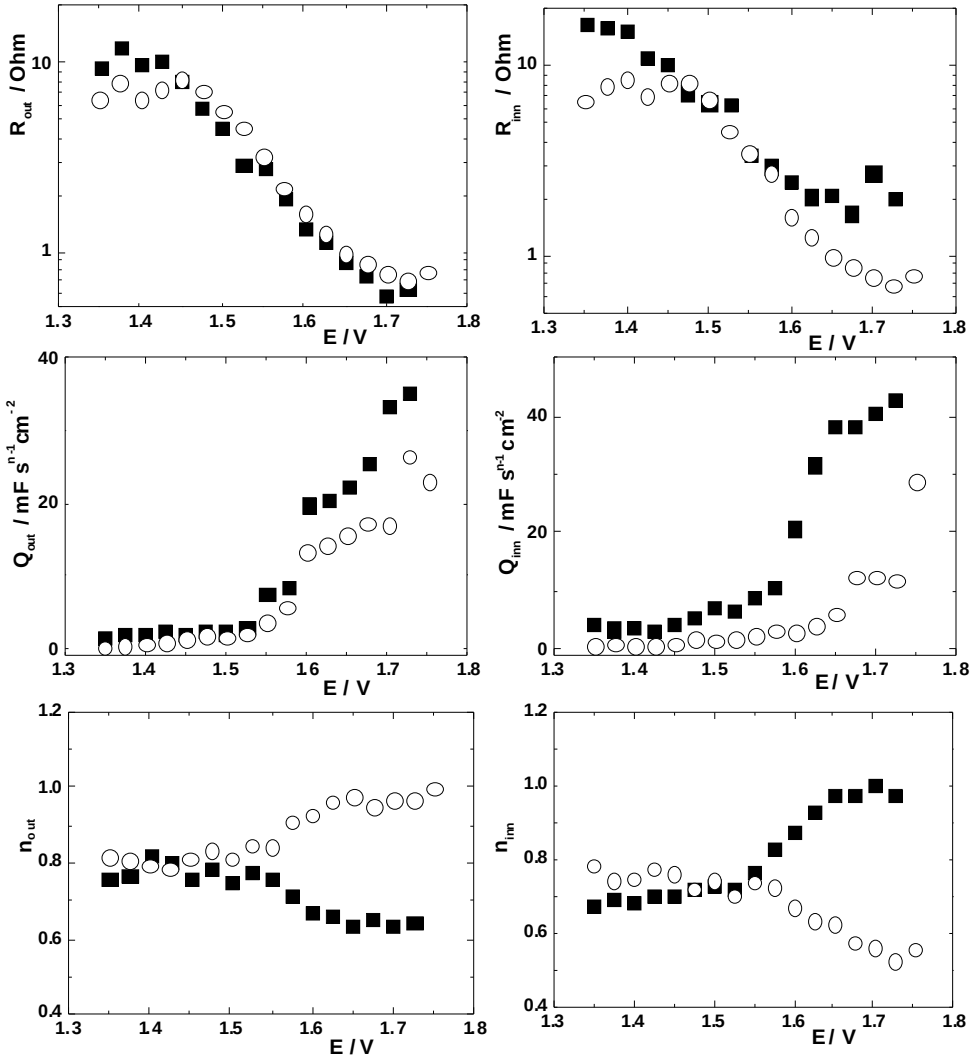

Figure 4: The fitted values of the equivalent circuit elements obtained for both inner and outer layer in dependence on the polarization potential of the FeC electrode at temperatures ■ 120 °C and ○ 160 °C.

4. Conclusions

Electrochemical way of ferrates(VI) preparation in molten hydroxide systems at low-temperature represents a “green” alternative to the other methods of ferrate(VI) production. Mossbauer spectroscopy proved the presence of ferrate(VI) at the electrode surface, furthermore colour changes of the electrolyte around the anode (dark violet colour) also supported this observation. Transpassive anodic dissolution of pure iron, silicon-rich steel and white cast iron, as electrode material, in molten sodium, potassium and KOH:KOH.H_2O eutectic mixture were carried out. Used electrochemical technique (cyclic voltammetry and electrochemical impedance spectroscopy) defined anodic potential region of ferrates(VI) production. It is close to the potential of oxygen evolution and it is treated as a parasitic anodic reaction in proposed potential window. For all systems the linear dependences of the anodic current density on square root of the polarization rate were found indicating that the electrode reaction kinetics is controlled by the mass

transport under the semi-infinitive linear diffusion conditions. In some cases the current density reaches a certain maximum, e.g. a chemical step due to the electrode structure become rate determining. This observation is in agreement with some previous results in the high-alkaline aqueous solutions observed by Macova et al. (2011, 2012). EIS was used to describe anode surface layers structure. Generally accepted model of two layer (outer and inner) sandwich structure was verified by impedance spectra characterised by two time constants. Both polarization resistances exhibit very similar values, which is in contrast with previous observations in aqueous highly-alkaline solutions (Hives et al., 2008b). This indicates rapid disruption of the passive-inner layer due to the higher temperature and electrolyte aggressivity. The decrease of the resistances of both sublayers is connected with their deterioration and thus its protective properties. This finding is important fact in design of the industrial process of ferrates(VI) production.

Acknowledgement

The authors gratefully acknowledge the financial support for this research by the Ministry of Education, Science, Research and Sport of the Slovak Republic within project VEGA 1/0985/12.

References

Hives J., Benova M., Bouzek K., Sharma V.K., 2006, Electrochemical formation of ferrate(VI) in a molten NaOH-KOH system, Electrochemistry Communications, 8, 1737-1740, DOI: 10.1016/j.elecom.2006.08.002

Hives J., Benova M., Bouzek K., Sitek J., Sharma V.K., 2008a, The Cyclic Voltammetric Study of Ferrate(VI) Formation in a Molten Na/K Hydroxide Mixture, Electrochimica Acta, 54, 203-208, DOI: 10.1016/j.electacta.2008.08.009

Hives J., Macova Z., Benova M., Bouzek K., 2008b, Comparison of the Ferrate(VI) Synthesis in the Eutectic NaOH – KOH Melt and Water Solution, J. Electrochemical Society, 155, E113-E119. DOI: 10.1149/1.2946716

Hrnciarikova L., Hives J., Kerekes K., Kamenar J., Gal M., 2010, Electrochemical behaviour of Fe and Fe-Si electrode in molten hydroxide mixture, Acta Chimica Slovaca 3, 74-83.

Macova Z., Bouzek K., Hives J., Sharma V.K., Terryn R.J., Baum J.C., 2009, Research progress in the electrochemical synthesis of ferrate(VI), Electrochimica Acta, 54, 2673-2683, DOI: 10.1016/j.electacta.2008.11.034

Macova Z., Bouzek K., Sharma V.K., 2010, The influence of electrolyte composition on electrochemical ferrate(VI) synthesis. Part I: anodic dissolution kinetics of pure iron, J. of Applied Electrochemistry, 40, 1019-1028, DOI: 10.1007/s10800-009-0051-8

Macova Z., Bouzek K., 2011, The influence of electrolyte composition on electrochemical ferrate(VI) synthesis. Part II: anodic dissolution kinetics of a steel anode rich in silicon, J. of Applied Electrochemistry, 41, 1125-1133, DOI: 10.1007/s10800-011-0332-x

Macova Z., Bouzek K., 2012, The influence of electrolyte composition on electrochemical ferrate(VI) synthesis. Part III: anodic dissolution kinetics of a white cast iron anode rich in iron carbide, J. of Applied Electrochemistry, 42, 615-626, DOI: 10.1007/s10800-012-0438-9

Sharma V.K., 2002, Potassium ferrate(VI): An environmentally friendly oxidant, Advances in Environmental Research, 6, 143-156, DOI: 10.1016/S1093-0191(01)00119-8